Drug Design, Development and Therapy

Dovepress
open access to scientific and medical research

Open Access Full Text Article

ORIGINAL RESEARCH

Gastro-Protective Effects of Calycosin Against Precancerous Lesions of Gastric Carcinoma in Rats

This article was published in the following Dove Press journal:
Drug Design, Development and Therapy

Danyan Li[1]
Luqing Zhao[1]
Yuxin Li[1,2]
Xiuhong Kang[1]
Shengsheng Zhang[1]

[1]Digestive Disease Center, Beijing Hospital of Traditional Chinese Medicine, Capital Medical University, Beijing, People's Republic of China; [2]Beijing University of Chinese Medicine, Beijing, People's Republic of China

Aim: Gastric cancer is a leading cause of cancer death worldwide. In-depth research of precancerous lesions of gastric carcinoma (PLGC) with malignant transformation potential is a key measure to prevent the development of gastric carcinoma. Recently, calycosin has been shown to have anticancer effects in vitro and in vivo. The molecular mechanism by which calycosin affects PLGC, however, has not yet been elucidated. The purpose of this study was to evaluate the effect and mechanism of calycosin in *N*-methyl-*N*′-nitro-*N*-nitrosoguanidine (MNNG)-induced PLGC rats.

Methods: The effects of calycosin in the gastric mucosa of rats with PLGC were evaluated using histopathology and transmission electron microscopy (TEM). For further characterization, the expression levels of integrin β1, nuclear factor kappa B (NF-κB), p-NF-κB, DARPP-32 and signal transducer and activator of transcription 3 (STAT3) were determined by Western blot assay and immunohistochemistry.

Results: Hematoxylin–eosin and high iron diamine–Alcian blue–periodic acid-Schiff (HID-AB-PAS) staining showed that intestinal metaplasia and dysplasia were significantly ameliorated in the calycosin intervention groups compared with the model group. Further, TEM results showed that calycosin intervention tempered microvascular abnormalities and cell morphology of primary and parietal cells in PLGC tissues. The results suggested that calycosin had gastro-protective effects in MNNG-induced PLGC rats. Western blot and immunohistochemistry analysis showed that the increased protein expression levels of NF-κB, p-NF-κB, DARPP-32 and STAT3 in the model group were downregulated by calycosin. The upregulation of integrin β1 expression induced by MNNG was decreased in the calycosin groups.

Conclusion: Collectively, calycosin protected against gastric mucosal injury in part via regulation of the integrin β1/NF-κB/DARPP-32 pathway and suppressed the expression of STAT3 in PLGC. The elucidation of this effect and mechanism of calycosin in PLGC provides a potential therapeutic strategy for treatment of gastric precancerous lesions.

Keywords: precancerous lesions of gastric carcinoma, calycosin, inflammation, angiogenesis, gastric mucosa protection

Introduction

Gastric cancer (GC) is the third leading cause of cancer death worldwide, having poor prognosis due to the lack of early detection and effective treatment modalities. Over 1,000,000 newly diagnosed cases and 783,000 deaths were estimated for 2018.[1] Early identification and prevention are important to reduce the socioeconomic burden associated with gastric cancer. It is well-known that human gastric carcinogenesis involves a cascade of mucosal changes: superficial gastritis → multifocal atrophic

Correspondence: Shengsheng Zhang
Digestive Disease Center, Beijing Hospital of Traditional Chinese Medicine, Capital Medical University, Beijing, People's Republic of China
Email zhss2000@163.com

submit your manuscript | www.dovepress.com
DovePress
http://doi.org/10.2147/DDDT.S247958

gastritis → intestinal metaplasia → dysplasia →gastric carcinogenesis.[2] The development of gastric precancerous lesions, which mainly depends on intestinal metaplasia and dysplasia,[3,4] is a critical stage in the evolution of gastric cancer.[5] Therefore, in-depth research of PLGC with malignant transformation potential is a key measure to prevent the development of gastric carcinoma.

Gastric mucosal intestinal metaplasia and dysplasia often occur as a result of inflammation. The relationship between inflammation and cancer was first proposed in the nineteenth century.[6] Although this connection has been out of favor for more than a century, interest in the relationship has gradually increased in recent years.[7,8] PLGC exactly reflects the "inflammation → cancer" transition. A study has shown that inflammation in the microenvironment has many tumor-promoting effects, including enhancement of proliferation and survival of malignant cells, and promotion of angiogenesis and metastasis.[9] This link between inflammation and cancer underscores the complexity of tumorigenesis, and the stage of PLGC provides a basis for research. Nuclear factor kappa B (NF-κB) is the central link of the inflammatory response and studies have shown that activation of NF-κB plays an important role in gastric cancer.[10] Blocking the signal transduction pathway to inhibit NF-κB may provide drugs for the treatment of malignant tumors.[11]

Integrins mediate interactions between tumor cells and the surrounding microenvironment and can regulate chronic inflammation and cancer-related pathological angiogenesis.[12] Only recently, integrin β1 has emerged as a key player in early pathogenic events in gastric carcinogenesis.[13] A very recent study showed that integrin β1 is involved in modulating NF-κB signaling pathway activity in GC, and silencing of integrin β1 decreased NF-κB signaling activation.[14] It has been reported that NF-κB regulates expression of DARPP-32 by binding directly to its promoter.[15] DARPP-32 overexpression can be detected in the early stages of the gastric cancer cascade, and research has shown that it may be involved in the transition from atrophic gastritis to intestinal metaplasia and tumor development.[16] Signal transducer and activator of transcription 3 (STAT3), a key transcription factor that has been shown to play a vital role in human gastric cancer angiogenesis,[17] is believed by some investigators to be directly involved in gastric tumorigenesis.[18] Although a number of molecular mechanisms involved in GC have been described over the years,[16] it is unclear what role these molecules may play in PLGC. Appropriate intervention for PLGC is urgently needed.

Calycosin, an isoflavonoid, is a major active component of *Astragalus membranaceus*, which is a traditional Chinese herbal medicine that has been widely used in the treatment of cancer, diabetic nephropathy and hepatic diseases.[19–21] Recently, several pharmacological studies have shown that calycosin can inhibit growth of human cancer cell lines, having impacts on cell proliferation, apoptosis and cell cycle distribution.[21–23] Emerging evidence suggests that calycosin can enhance cisplatin-induced suppression of a gastric cell line.[24] However, the effects of calycosin on gastric mucosa protection in PLGC are unclear. Hence, investigation of the effects of calycosin on progression of gastric precancerous lesions may provide novel insights into the development of therapeutic agents.

In this study, a rat model of N-methyl-N′-nitro-N-nitrosoguanidine (MNNG)-induced PLGC was used for experiments. The effects of calycosin in the treatment of PLGC and its potential mechanism of action were explored.

Methods and Materials

Animals

Sixty male Sprague-Dawley (SD) rats aged 4–6 weeks were obtained from Vital River Laboratories Animal Technology Co., Ltd. Beijing, China (Certification No. SCXK (Beijing) 2016–0002). The protocol was designed to minimize discomfort to the animals. All rats were maintained in specific pathogen-free conditions with a 12 h light-dark cycle, room temperature of 20–26°C, and relative humidity of 40–70% in the animal facility of Beijing Institute of T.C.M. The rats had free access to regular chow diet and water. The present study was performed in accordance with the Guide for the Care and Use of Laboratory Animals published by the National Institutes of Health, and was approved by the Animal Care and Use Committee of Beijing Institute of Traditional Chinese Medicine (no. 2,018,120,103).

Experimental Design

Following 1 week acclimation, the rats were randomly divided into control (n = 15) and intervention (n = 45) groups. The number of animals used in the study was based on reference to published articles.[25–27] As described in the literature, MNNG was administered to the rats in the intervention group via drinking water at a concentration of 200 μg/mL in light-shielded bottles and the rats were fed normal diet every other day.[25–27] The administration was conducted for 16 weeks as described in the literature. Rats in the control group had free access to food and water. At 8, 12, and 16

weeks, three rats were randomly sacrificed from the intervention group to perform histological evaluation. According to the histological evaluation, rats in the intervention group exhibited intestinal metaplasia or dysplasia in week 16. The intervention group was then randomly divided into three groups: model group, calycosin low dose (Calycosin L) group (n = 12, 40 mg/kg) and calycosin high dose (Calycosin H) group (n = 12, 80 mg/kg). The PLGC rats were dosed with calycosin for 10 weeks (Figure 1). At the end of the experiment (26 weeks), all rats were fasted for 12 h and then euthanized with 1% pentobarbital sodium.

Antibodies and Reagents

Calycosin (purity > 98%) and MNNG were purchased from Wanxiang Hengyuan Technology Co., Ltd. (Tianjin, China) and Tokyo Chem. Ind. (Shanghai, China), respectively. Anti-integrin β1 (ab179471), anti-DARPP-32 (ab40801), anti-NF-κB (ab16502) and anti-p-NF-κB (ab86299) antibodies were purchased from Abcam, Shanghai, China. STAT3 (#9139) antibody was purchased from Cell Signaling Technology, Inc., Shanghai, China. The BCA kit was purchased from Solarbio Science & Technology Co., Ltd., Beijing, China.

Histopathological Observation

Gastric tissue samples from each group were collected and fixed in 10% neutral-buffered formalin overnight, and then dehydrated in alcohol and xylene, successively. Dehydrated samples were embedded in paraffin and sectioned into 4 μm slices. This was followed by staining with hematoxylin and eosin (H&E) dye using standard techniques to observe morphological changes. High iron diamine–Alcian blue–periodic acid–Schiff (HID-AB-PAS) staining was performed to detect types of intestinal metaplasia according to the manufacturer's introductions. The sections were observed and analyzed using light microscopy (Nikon, Chiyoda-Ku, Tokyo, Japan) at 100×, 200× and 400× magnification and photographed.

Ultrastructure Observation

The ultrastructure of the gastric mucosa was evaluated by transmission electron microscopy (TEM). Gastric tissue samples from each group were sliced into 1 mm^3 pieces and fixed with 2.5% glutaraldehyde at 4°C overnight. The tissue samples were then post fixed in 1% osmium tetroxide for 2 h, dehydrated in a graded series of ethanol solutions, and then immersed twice in a mixture of acetone and epoxy resin. Finally, the tissues were embedded in epoxy resin-filled capsules and heated at 70°C overnight. Ultrathin sections (60–80 nm) were cut using an ultramicrotome, followed by staining with uranyl acetate and lead citrate. Images were captured by TEM (HT7700, Tokyo, Japan) and used to describe the ultrastructure of gastric epithelial cells.

Western Blotting

Stomach tissues were ground in liquid nitrogen, homogenized on ice using lysis buffer containing protease inhibitors, and centrifuged at 12,000 rpm for 15 min to obtain the supernatant. Protein concentrations were quantified using a BCA protein assay kit (Solarbio Science & Technology Co., Ltd., Beijing, China). Equal amounts of proteins were loaded onto the SDS-PAGE gel electrophoresis system and the separated bands were transferred onto PVDF membrane (Millipore, Bedford, MA, USA). The membrane was blocked with 5% nonfat milk for 1 h at room temperature, and then incubated at 4°C overnight with anti-integrin β1 (1:2000; ab179471, Abcam), anti-NF-κB (1:2000; ab16502, Abcam), anti-p-NF-κB (1:2000; ab86299, Abcam), anti-DARPP-32 (1:1000; ab40801, Abcam), and anti-STAT3 (1:1000; #9139, Cell Signaling Technology, Inc.) primary antibodies. Electrophoresis of anti-DARPP-32 was conducted with 12% gel, while 10% gel was used for the other antibodies. Subsequently, the membranes were washed and incubated with secondary antibodies for 1 h at room temperature. Routinely, protein load was monitored by using

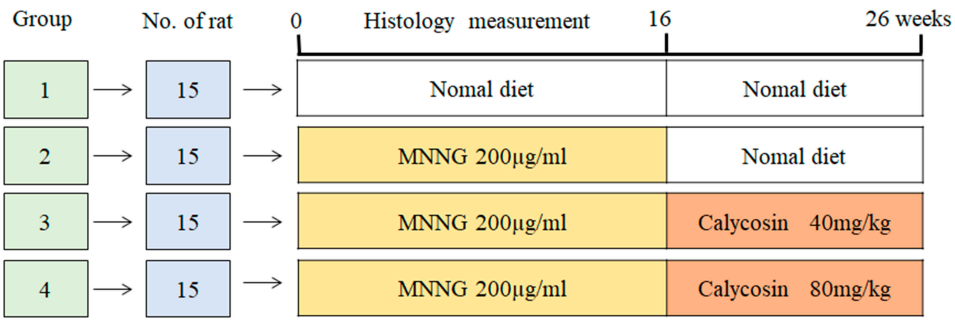

Figure 1 Experimental design scheme.

a super enhanced chemical luminescence reagent (ECL; Millipore, Bedford, MA, USA). The polypeptide bands from Western blotting were quantified by Image-J 1.46r software (National Institutes of Health, Bethesda, MD, USA), and normalized to GAPDH or actin (loading control).

Immunohistochemistry

Stomach tissue sections were fixed in 4% paraformaldehyde at room temperature, embedded in paraffin, cut into 4 μm slices and mounted on glass slides. The sections were heated to 60°C for 20 min, de-paraffinized in xylene and dehydrated in alcohol. Antigen retrieval was performed in a pressure cooker using sodium citrate buffer (pH 6.0). The sections were then soaked in 3% H_2O_2/methanol solution to inhibit endogenous peroxidase activity, and then blocked with 3% bovine serum albumin (BSA). The sections were incubated overnight at 4°C with anti-DARPP-32 (1:50; ab40801, Abcam) and anti-STAT3 (1:300; #9139, Cell Signaling Technology, Inc.) primary antibodies. After washing for 10 min in phosphate buffered saline (PBS, pH 7.4), the sections were incubated for 20 min in horseradish peroxidase (HRP)-labeled secondary antibody, goat anti-rabbit or goat anti-mouse IgG (1:200; GB2301 and GB23303, Wuhan Servicebio Technology Co., Ltd.), and for 1 min in DAB reagent. The sections were then counterstained with hematoxylin prior to dehydration with ethanol and xylene. Images were obtained using a light microscope at 100×–200× magnification (Carl Zeiss AG), and the immunoreactivities of DARPP-32 and STAT3 were determined using Image Pro Plus 6.0 image analysis software (Media Cybernetics, Inc.).

Statistical Analysis

All results were expressed as mean ± standard deviation (SD). A *t*-test or ANOVA was conducted if the quantitative data were of normal distribution and homogeneity of variance, otherwise a Kruskal–Wallis rank sum test was conducted. Results were considered to be of statistically significant difference at $P < 0.05$, and $P < 0.01$ indicated that the difference was of high significance. All statistical analyses were conducted using Graphpad Prism 6.0 (Graphpad Software, CA, USA).

Results

Animal Model

The PLGC animal model was established by giving MNNG and normal diet every other day. In the 8th, 12th, and 16th weeks, histological observation of gastric mucosal lesions was evaluated by H&E staining. Data in the model group showed that MNNG induced significant alterations in gastric gland morphology (Figure 2). Compared with histopathology of gastric mucosa in control rats (Figure 2A and E), individual vacuolar lesions in gastric mucosa epithelium, and hyperchromatic nuclei in some gastric epithelial cells were observed in the 8th week (Figure 2B and F). In the 12th week, increased vacuolar lesion changes and irregular gland arrangement were observed (Figure 2C and G). In the 16th week, the presence of diffuse vacuolar lesions and significantly irregular arrangement, together with hyperchromatic and nuclear alterations, confirmed intestinal epithelial metaplasia and gastric gland dysplasia (Figure 2D and H). The PLGC model was satisfactorily established at the end of week 16.

Routine Pathology Evaluation

At the end of the 26th week, macroscopic and microscopic lesions in the gastric mucosa were recorded. As shown in Figure 3, compared to the control group, pale gastric mucosa, hyperemia and sporadic erosion were observed in the model group and elasticity of the gastric wall was decreased. After treatment with calycosin, the poor elasticity of the gastric wall and the flat gastric mucosa folds were ameliorated compared with the model rats.

H&E staining was used to examine histopathological changes of the gastric mucosa. Compared with the control group (Figure 4A and E), obvious pathological changes were found. The gland arrangement of the gastric mucosa in the model group was irregular and crowded (Figure 4B and F). In addition, the gastric epithelial cells exhibited increased nuclear-cytoplasmic ratio, loss of nuclear polarity, hyperchromatic and crowded nuclei, and cavity fusion of the gastric mucosa was stimulated. These results indicated that dysplasia with intestinal metaplasia was present in the gastric mucosa. Interestingly, a PLGC-rescuing effect was observed in calycosin-treated rats. The area of dysplastic gastric epithelial cells and inflammatory infiltration was decreased (Figure 4C, D, G and H). These observations suggested that calycosin protected the gastric mucosa in MNNG-induced PLGC rats.

Staining with HID-AB-PAS was used to evaluated the degree of intestinal metaplasia in gastric tissues. As shown in Figure 5, neutral mucins present in normal mucosa were stained red, while gastric specimens from controls were not stained (Figure 5A and E). In the model group, mucosal metaplasia tissue was positively stained, and intestinal metaplasia cells were located on the gastric cavity side and in the lamina propria (Figure 5B and F). Interestingly, intestinal

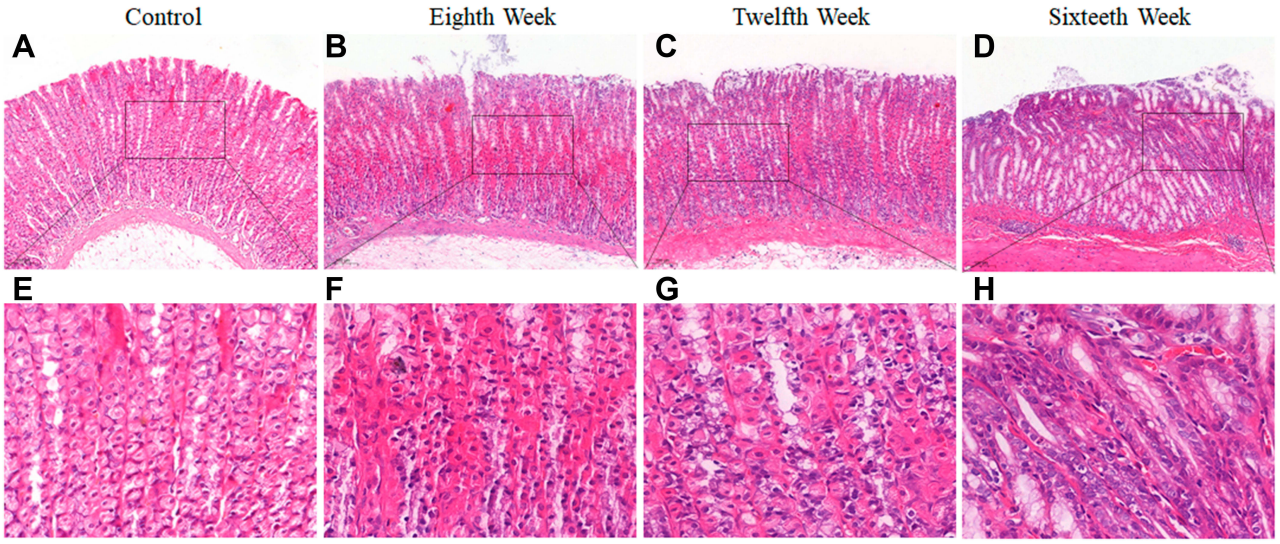

Figure 2 Histopathological changes of gastric mucosa following administration of *N*-methyl-*N'*-nitro-*N*-nitrosoguanidine (MNNG) for 8, 12 and 16 weeks. (**A** and **E**) Histopathological changes of gastric mucosa in the control group (H&E staining, 10×, 40×). (**B** and **F**) Histopathological changes of gastric mucosa in the 8th week (H&E staining, 10×, 40×). (**C** and **G**) Histopathological changes of gastric mucosa in the 12th week (H&E staining, 10×, 40×). (**D** and **H**) Histopathological changes of gastric mucosa in the 16th week (H&E staining, 10×, 40×).

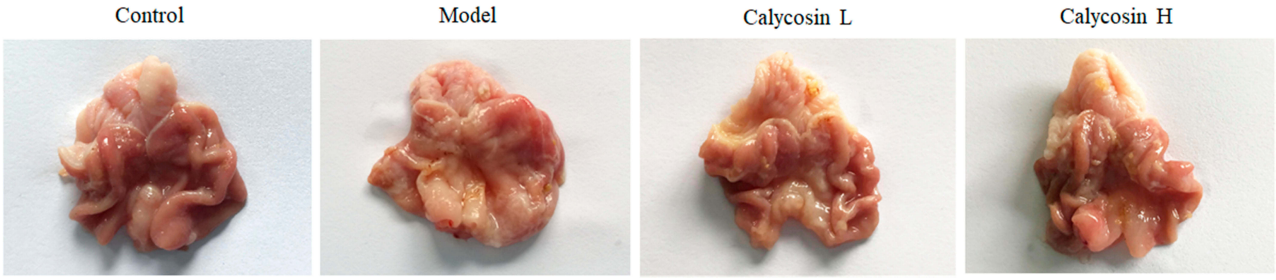

Figure 3 Macroscopic changes of gastric mucosa in different groups after 26 weeks.

metaplasia was regressed visibly in calycosin-treated rats compared with the model rats (Figure 5C, D, G, and H). Our observations revealed potent activity of calycosin against intestinal metaplasia in PLGC rats.

Transmission Electron Microscopy (TEM) Analysis

In the control group, normal cell morphology was observed in primary and parietal cells. At the same time, the endoplasmic reticulum, mitochondria and Golgi complex were of regular shape. Rich zymogen particles were visible in the cytoplasm of the chief cells.

In the model group, the chief cell nucleus was irregular in shape, depressed, nuclear chromatin was concentrated, and there was a high proportion of nuclear matter. The secretion of zymogen particles was reduced, and the boundary membrane between zymogen particles was not clear. Secretory tubules were dilated in parietal cells, and lumen microvilli were fewer in number, deformed, and suffered from mitochondrial swelling and spasm. There were also fewer rough endoplasmic reticulum and Golgi complexes in the cells.

In the high dose group, the cytoplasm of the chief cell contained an abundance of zymogen particles. The number of dilated secretory tubules in parietal cells was reduced and the number of microvilli was increased. The number of Golgi complexes increased slightly, the endoplasmic reticulum increased, with no obvious expansion, and the number and density of mitochondria increased. In the low-dose group, the cytoplasm of the chief cell contained an abundance of zymogen granules, the nuclear membrane and cytoplasmic gap were slightly widened, and the microvilli in the lumen of the secretory tubules were increased in the parietal cells. There were more mitochondria in the

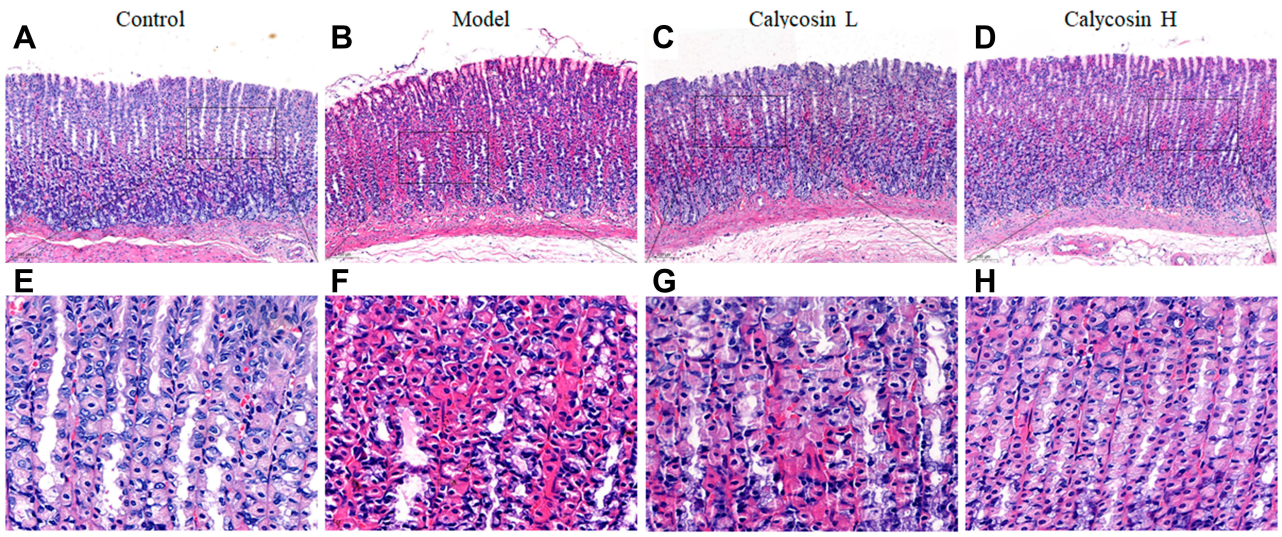

Figure 4 Effects of calycosin on histopathological changes in the gastric mucosa of PLGC rats. (**A** and **E**) Histopathological changes of gastric mucosa in the control group (H&E staining, 10×, 40×). (**B** and **F**) Histopathological changes of gastric mucosa in the model group (H&E staining, 10×, 40×). (**C** and **G**) Histopathological changes of gastric mucosa in the calycosin low group (H&E staining, 10×, 40×). (**D** and **H**) Histopathological changes of gastric mucosa in the calycosin high group (H&E staining, 10×, 40×).

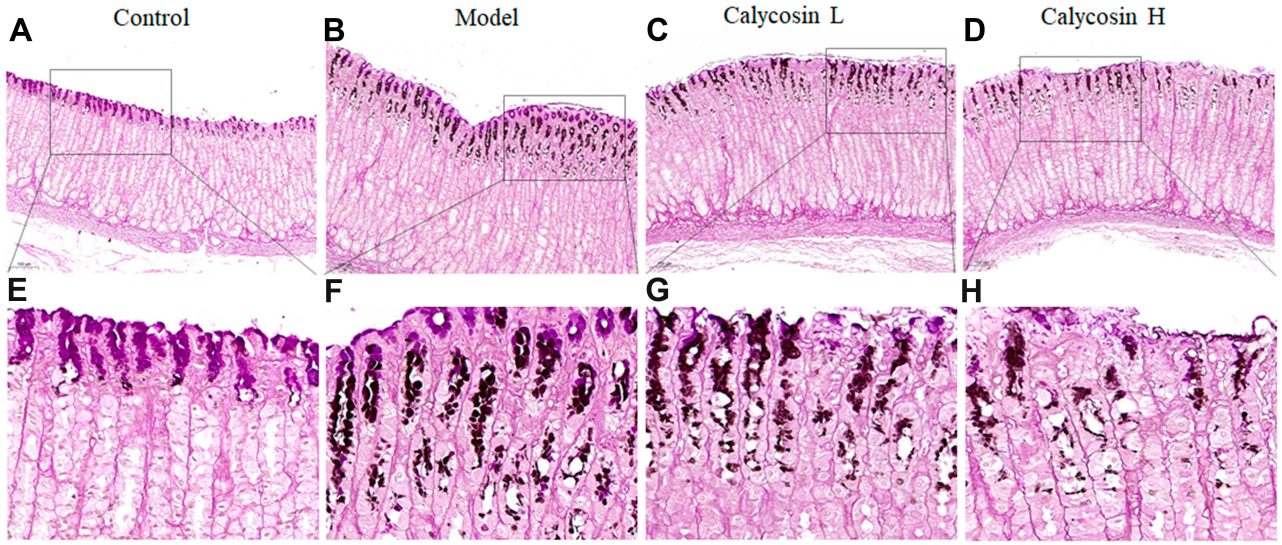

Figure 5 Effects of calycosin on histopathological changes in gastric mucosa tissue of PLGC rats. (**A** and **E**) Histopathological changes of gastric mucosa in the control group (HID-AB-PAS staining, 10×, 40×). (**B** and **F**) Histopathological changes of gastric mucosa in the model group (HID-AB-PAS staining, 10×, 40×). (**C** and **G**) Histopathological changes of gastric mucosa in the calycosin low group (HID-AB-PAS staining, 10×, 40×). (**D** and **H**) Histopathological changes of gastric mucosa in the calycosin high group (HID-AB-PAS staining, 10×, 40×).

cells, and the number of endoplasmic reticulum increased slightly (Figure 6A and B).

In addition, we analyzed the effect of calycosin on vascular structure in MNNG-PLGC rats. As shown in Figure 6C, normal vascular inner diameter, smooth basal lamina and intact basement membrane were observed in control rats. In contrast, the basal lamina in model rats was rough and the basement membrane was irregular and discontinuous. Features such as segmental rupture of the basal cavity and increased vascular permeability were also observed. Apart from these, endothelial cells displayed nuclear chromatin condensation. In calycosin-treated rats, the basal lamina was still a little rough but the basement membrane tended to be intact. Both basal lamina and basement membrane were

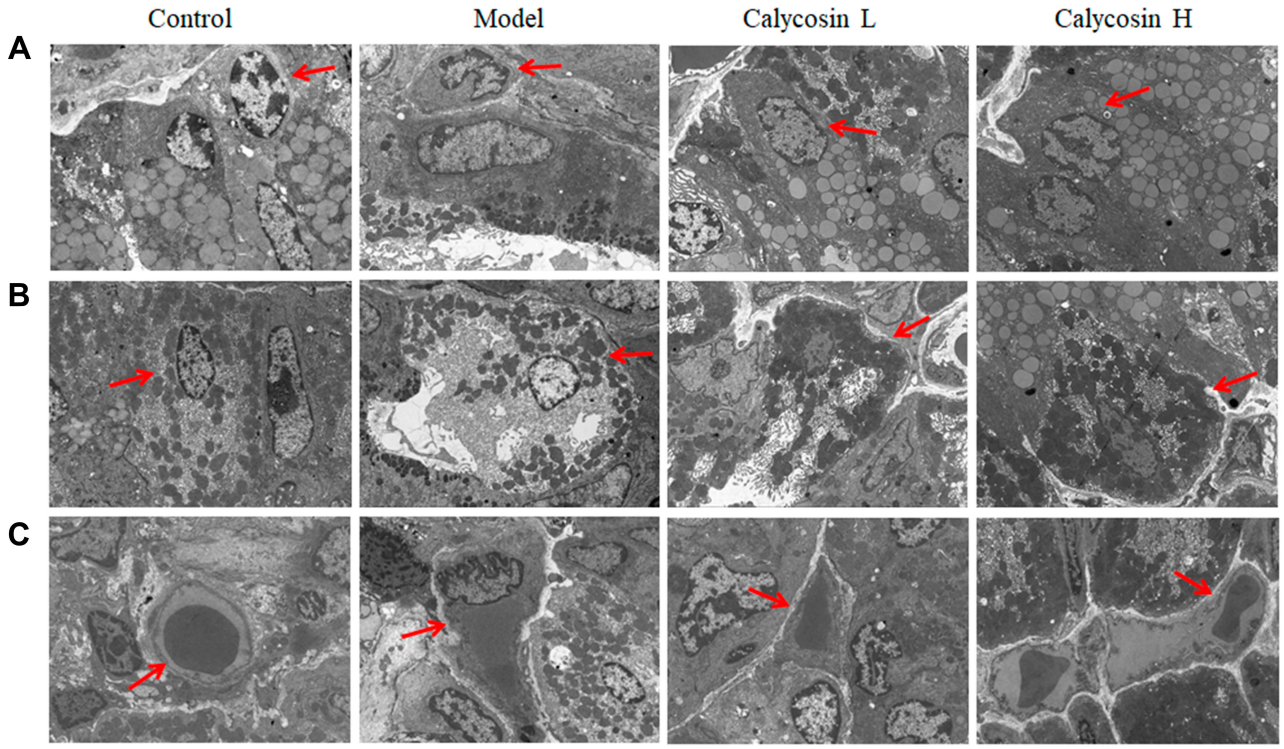

Figure 6 Effects of calycosin on ultrastructural changes in gastric mucosa of PLGC rats. (**A**) The ultrastructure of chief cells in gastric mucosa (2.5k×), and the red arrow represents chief cells. (**B**) The ultrastructure of parietal cells in the gastric mucosa (2.5k×), and the red arrow represents parietal cells. (**C**) The microvessel ultrastructure in gastric mucosa (2.5k×), and the red arrow represents microvessel.

improved compared with the model group. This suggested that calycosin intervention tempered microvascular abnormalities in PLGC tissues, exhibiting a potent protective effect against MNNG-induced vascular damage.

Measurement of Integrin β1, NF-κB, p-NF-κB, DARPP-32 and STAT3 Protein Expression

To further evaluate the effects of calycosin, we investigated the role of integrin β1, NF-κB, p-NF-κB, DARPP-32 and STAT3 in PLGC inflammation and angiogenesis. As reported in the literature, NF-κB is highly expressed in gastric cancer,[15] and integrin β1 is involved in activation of NF-κB signaling. Silencing of integrin β1 led to inhibition of NF-κB signaling.[14] We speculated that integrin β1 and NF-κB were also highly expressed in gastric precancerous lesions. As shown in Figure 7B, D and E, protein expression levels of NF-κB and p-NF-κB were upregulated in MNNG-induced rats compared to the control group, and the level of integrin β1 was markedly increased ($^{\#}P < 0.05$, Figure 7A and C). Levels of NF-κB and p-NF-κB were decreased after 10 weeks of treatment with both doses of calycosin in a dose-dependent manner ($^{*}P < 0.05$).

Furthermore, it has been reported that DARPP-32 is a marker of blood vessels, endothelial cells and indicative of angiogenesis,[28] and that DARPP-32 is more highly expressed in tumors, including gastric cancer.[29,30] STAT3 is a transcription factor that is involved in various cellular responses. We investigated whether STAT3 was activated in MNNG-PLGC rats, and what role DARPP-32 and STAT3 might play in PLGC rats. As shown in Figure 8, statistically significant increases of DARPP-32 and STAT3 expression were observed in model rats when compared with the control group ($^{\#}P < 0.05$), while calycosin treatment downregulated their levels when compared with levels in non-treated rats ($^{*}P < 0.05$, Figure 8A–D). Moreover, immunohistochemistry (IHC) staining of DARPP-32 and STAT3 expression gave the same results (Figure 9A–C).

These findings demonstrated the presence of inflammation and angiogenesis in PLGC, partly due to increased expression of NF-κB, DARPP-32 and STAT3, which could have a role in the pathogenesis of PLGC. Calycosin alleviated the overexpression of NF-κB, DARPP-32 and STAT3, possibly due to downregulation of integrin β1.

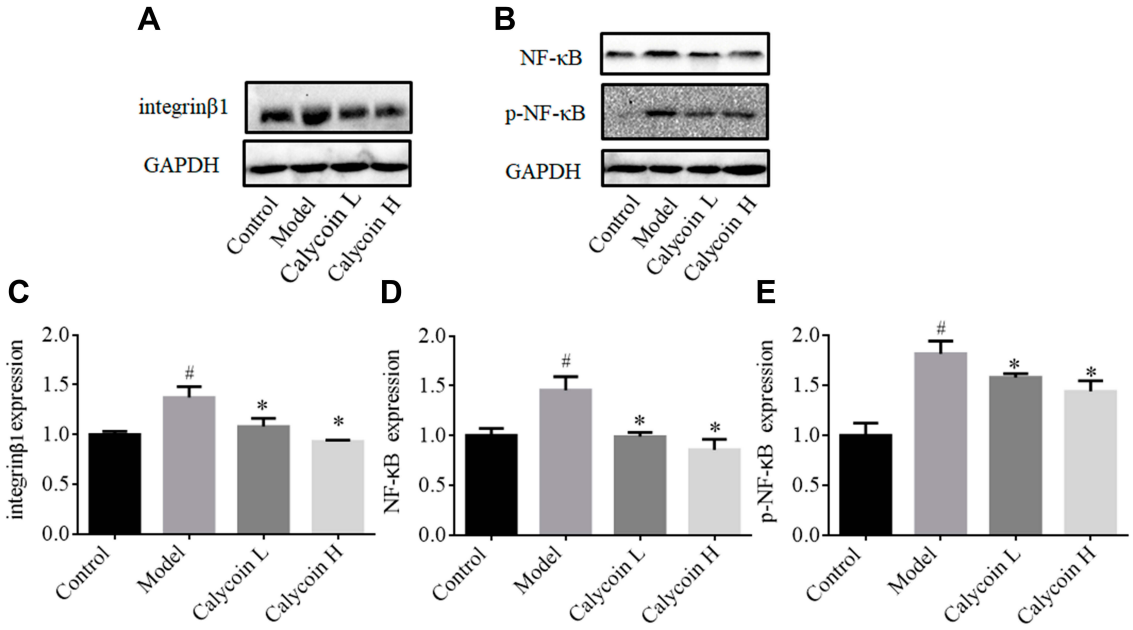

Figure 7 Effects of calycosin on integrin β1, NF-κB, and p-NF-κB in the gastric mucosa of PLGC rats. (**A** and **B**) Western blot analysis of integrin β1, NF-κB, and p-NF-κB protein levels in PLGC groups after treatment with calycosin. (**C**–**E**) Quantitative analysis of integrin β1 (**C**), NF-κB (**D**) and p-NF-κB (**E**). Expression was standardized to GAPDH expression. Data are shown as the mean ± SD (n = 3 rats per group). $^{\#}P < 0.05$ versus the control group. $^{*}P < 0.05$ versus the model group.

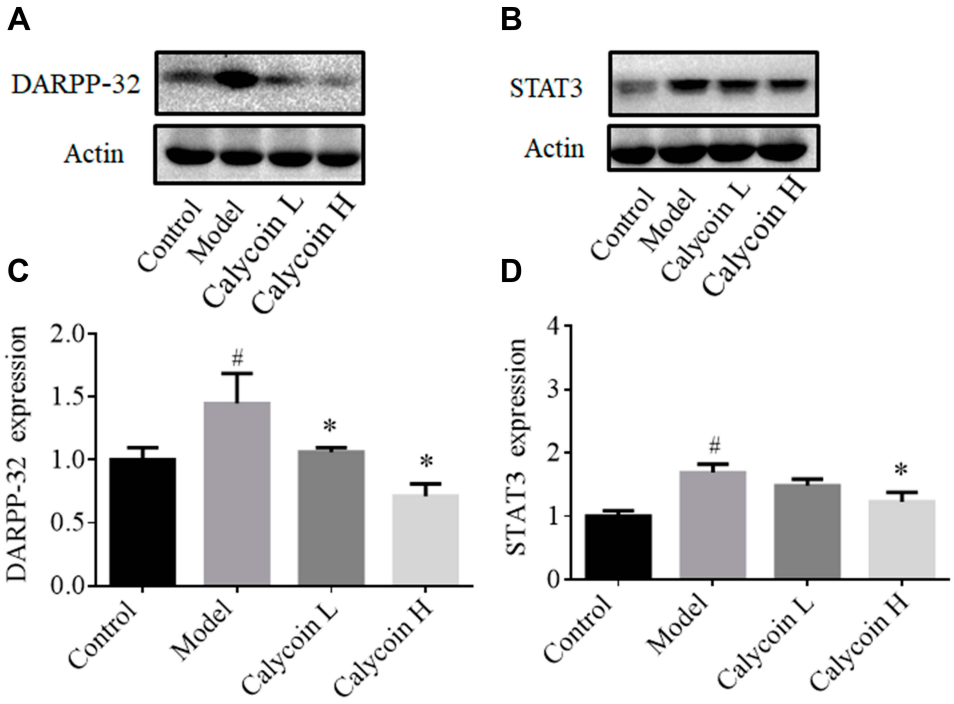

Figure 8 Effects of calycosin on DARPP-32, and STAT3 expression in gastric mucosa of PLGC rats. (**A** and **B**) Western blot analysis of DARPP-32 and STAT3 protein levels in PLGC groups after treatment with calycosin. (**C** and **D**) Quantitative analysis of DARPP-32 (**A**) and STAT3 (**B**). Expression was standardized to actin expression. Data are shown as the mean ± SD (n = 3 rats per group). $^{\#}P < 0.05$ versus the control group. $^{*}P < 0.05$ versus the model group.

Discussion

It is well established that the presence of premalignant changes of the gastric mucosa is an important risk factor for development of gastric cancer.[31] Early intervention, therefore, for gastric precancerous lesions is important to reduce the morbidity of gastric cancer.[32] Calycosin is a product isolated

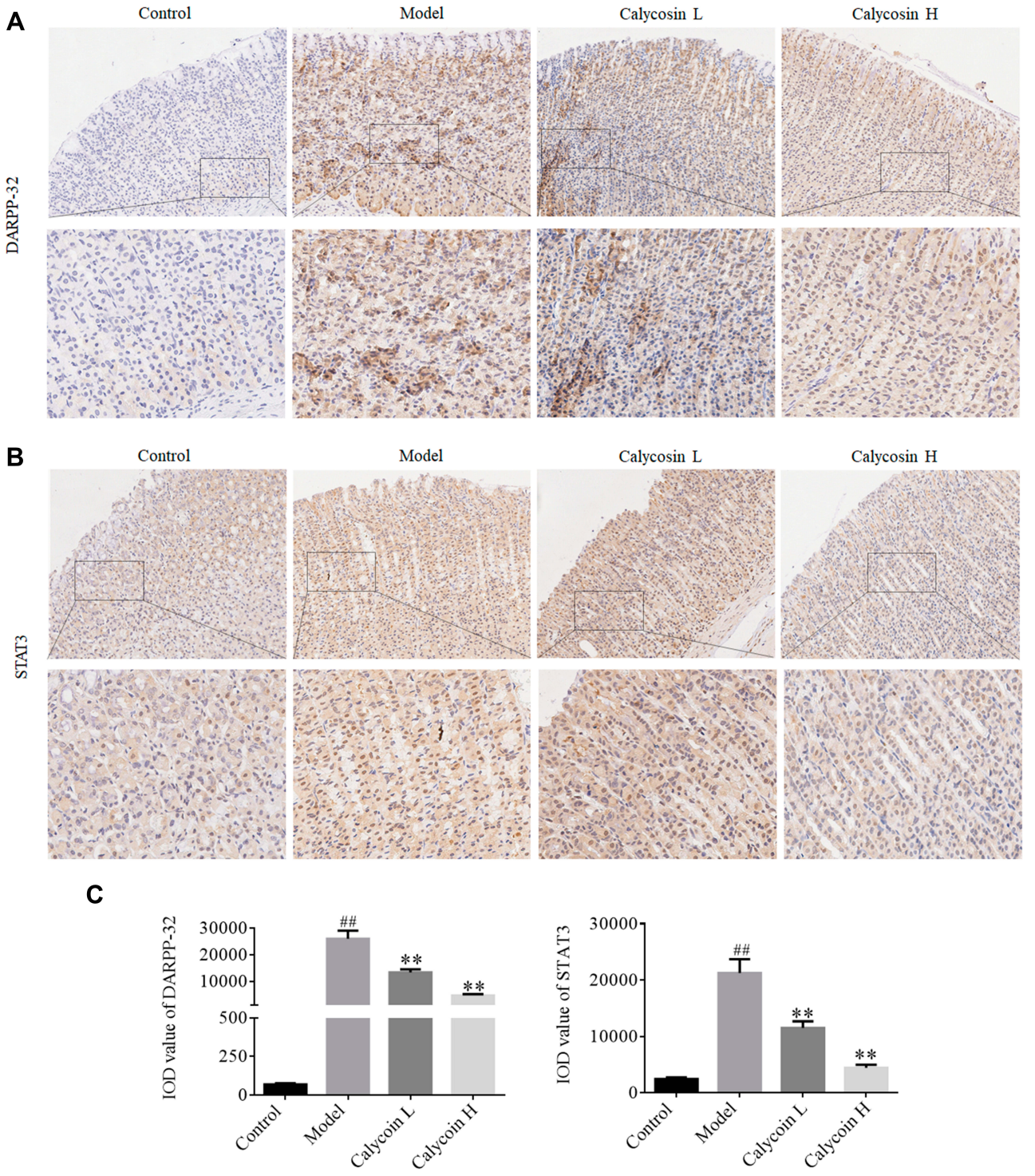

Figure 9 (**A**) Expression of DARPP-32 in gastric mucosa of each group detected by IHC staining (20×, 40×). (**B**) Expression of STAT3 in gastric mucosa tissue of each group detected by IHC staining (20×, 40×). (**C**) Immunohistochemical expression of DARPP-32 and STAT3 shown as IOD value, which was determined by Image-Pro Plus. Data are shown as the mean ± SD (n = 3 rats per group). $^{\#\#}P < 0.01$ versus the control group. $^{**}P < 0.01$ versus the model group.
Abbreviation: IOD, integrated optical density.

from *Astragalus membranaceus* Bge., a Chinese traditional herb that has a long history of use as a medicine. In recent years, many basic and clinical studies have shown that calycosin has anti-cancer effects. However, there is no report on the effects of calycosin on gastric precancerous lesions. In the present study, morphological and histopathological changes of gastric epithelial cells were apparent in the PLGC rat model. An interesting aspect of our study was that the

physiopathology was attenuated by treatment with calycosin, suggesting that the compound reversed MNNG-induced PLGC by protecting the gastric mucosa.

Integrin β1 plays an important role in cell signaling, differentiation, migration and apoptosis, all processes that are essential for the evolution and development of gastric carcinogenesis.[13] Increasing evidence associates high levels of integrin β1 expression with poor prognosis and recurrence in patients with gastric carcinoma.[33,34] Several studies have demonstrated the correlation of integrin β1 expression with malignant features.[35–37] Consistent with the reported expression of integrin β1 in cancers, we found that its level was significantly increased in MNNG-induced PLGC. Levels of integrin β1 were markedly decreased in the calycosin treatment group. NF-κB is the central link of the inflammatory response that can promote inflammatory infiltration and alter expression of inflammatory cytokines.[38] Upregulation of NF-κB has been suggested to promote development and progression of gastric carcinoma.[39] In the present study, our results showed that calycosin decreased the upregulated expression of NF-κB and p-NF-κB induced by MNNG. Our results were consistent with the presence of persistent inflammation in the development of PLGC and progression to gastric carcinoma.[40] Further, a very recent study showed that integrin β1 was involved in modulating NF-κB signaling pathway activity in gastric carcinoma, and silencing of integrin β1 decreased NF-κB signaling activation.[14] Inhibition of integrin β1 has also been shown to abrogate formation of metastases in gastric models.[41] Thus, calycosin may reverse PLGC by regulating integrin β1 and the NF-κB signaling pathway.

DARPP-32, a critical factor of blood vessels and endothelial cells that is indicative of angiogenesis, participates early in the transition from atrophic gastritis to intestinal metaplasia and dysplasia, and persists in the subsequent progression of gastric tumorigenesis.[42,43] DARPP-32 is a frequently overexpressed protein that promotes several oncogenic functions in gastric cancer.[28,42] In gastric cancer cell lines, DARPP-32 was found to be regulated by NF-κB,[15] which has recently been shown to be activated and can promote a proinflammatory environment, inhibit apoptosis and stimulate cell proliferation.[44] Of note, this study found that DARPP-32 expression was upregulated in MNNG-induced PLGC rats, indicating that angiogenesis was occurring. Consistent with gastric carcinogenesis, the activation of the NF-κB/DARPP-32 pathway is involved in the progression of PLGC. Protein levels of DARPP-32, one of the critical downstream genes of NF-κB, were increased in the model group and downregulated in the calycosin treatment group. Taken together, these results suggested that the therapeutic effects of calycosin may be mediated in part by modulation of the integrin β1/NF-κB/DARPP-32 pathway in MNNG-induced PLGC rats (Figure 10).

Furthermore, consistent with the proposed link between inflammation and angiogenesis, STAT3 has been implicated in tumor angiogenesis in many human cancers.[45,46] Numerous investigations have shown that the activities of STAT3 and NF-κB are elevated in many cancers.[47,48] Our results showed that STAT3 and NF-κB protein levels were increased in the PLGC model group, consistent with the published literature.[49] STAT3 nuclear translocation was observed by immunohistochemistry staining. Normally, STAT3 is activated for a short time and then deactivated to maintain homeostasis; under abnormal conditions, persistent STAT3 activation triggers oncogene transcription.[50] We speculated that chronic inflammation may constitute abnormal conditions. Our results showed high expression of p-NF-κB in PLGC model rats. Studies have demonstrated that p-NF-κB induces expression of genes involved in inflammation, such as IL-6.[38] Evidence has shown that the IL-6/STAT3 signaling pathway completes the link between inflammation and cancer.[51] In other words, NF-κB activation is a manifestation of inflammation or the consequence of an inflammatory microenvironment formed during malignant progression.[52] Inflammation may be a prominent inducer, and later lead to microvascular injury,[53] driving angiogenesis by direct and indirect mechanisms to promote endothelial proliferation and vessel sprouting.[54] Studies have demonstrated that inhibition or knockdown of STAT3 suppressed angiogenesis in different human cancers.[55–57] In this study, calycosin downregulated STAT3 levels when compared with levels in non-treated rats. The data suggest that calycosin may act in part via inhibition of integrin β1/NF-κB signaling, later suppressing STAT3 expression, in MNNG-induced PLGC rats.

Perhaps the most interesting aspect of these studies was that the expression levels of integrin β1, NF-κB, DARPP-32 and STAT3 in the model provided in vivo support for the link between NF-κB activation, inflammation, and angiogenesis in PLGC. If intestinal metaplasia and dysplasia are the "match that lights the fire" of gastric carcinoma, angiogenesis and some types of uncontrolled inflammation may provide the "fuel that feeds the flames".

In summary, the study mainly focused on the protective effect of calycosin against PLGC. Calycosin is derived from a traditional tonic herb, *Astragalus membranaceus*.[58] It is a flavonoid, which is a class of compounds that have broad spectrum pharmacological activities as well as toxicity.

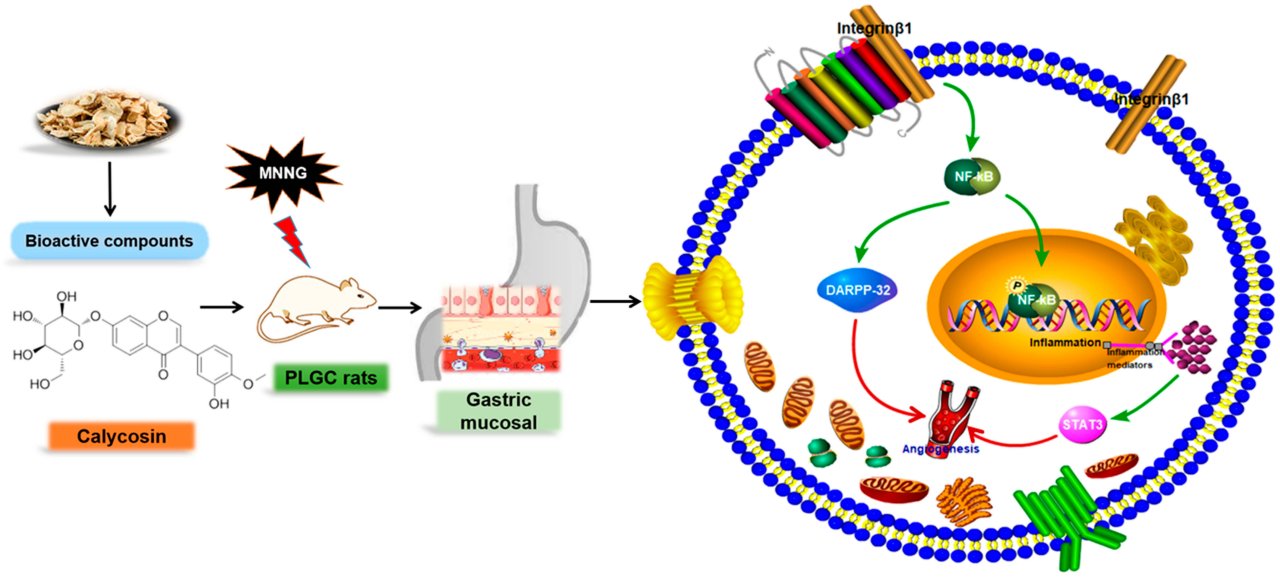

Figure 10 Summary of the molecular effects of calycosin. Calycosin protected gastric mucosa by regulating the integrin β1/NF-κB/DARPP-32 pathway and decreasing STAT3 expression in MNNG-induced PLGC rats. The green arrow represents the promotion, and the red arrow represents the direction of the final result.

Studies have shown that flavonoids decreased both iodide ion uptake and incorporation and are associated with thyroid diseases.[59,60] With respect to the toxicity of calycosin, our previously published results from in vivo experiments demonstrated that intravenous calycosin significantly suppressed the growth of established glioblastoma xenografts without causing any loss in body weight. Calycosin exhibited relatively low toxicity toward normal tissues.[23] Research and application of natural products requires attention to not only positive but also negative biological effects and mechanisms. We will further focus on the specific toxic effects of calycosin in future studies.

Conclusion

In conclusion, the mechanism for the gastro-protective effect of calycosin may be associated with regulation of the integrin β1/NF-κB/DARPP-32 pathway and suppression of STAT3 expression in MNNG-induced PLGC rats. With increased interest in this pathway, it can be anticipated that numerous pharmacological inhibitors may be developed with promising prospects for treatment of patients with PLGC.

Acknowledgments

This research was supported by Beijing Postdoctoral Foundation (No. ZZ2019-24) and Beijing Administration of Traditional Chinese Medicine "Yanjing School Innovative Inheritance Fist Project".

Disclosure

The authors declare that they have no competing interests.

References

1. Bray F, Ferlay J, Soerjomataram I, et al. Global cancer statistics 2018: GLOBOCAN estimates of incidence and mortality worldwide for 36 cancers in 185 countries. *CA Cancer J Clin*. 2018;68(6):394–424. doi:10.3322/caac.21492
2. Correa P. A human model of gastric carcinogenesis. *Cancer Res*. 1988;48:3554–3560.
3. de Vries AC, van Grieken NC, Looman CW, et al. Gastric cancer risk in patients with premalignant gastric lesions: a nationwide cohort study in the Netherlands. *Gastroenterology*. 2008;134:945–952. doi:10.1053/j.gastro.2008.01.071
4. Yoon H, Kim N. Diagnosis and management of high risk group for gastric cancer. *Gut Liver*. 2015;9:5–17. doi:10.5009/gnl14118
5. Huang L, Wu RL, Xu AM. Epithelial-mesenchymal transition in gastric cancer. *Am J Transl Res*. 2015;7:2141–2158.
6. Balkwill F, Mantovani A. Inflammation and cancer: back to Virchow? *Lancet*. 2001;357:539–545. doi:10.1016/S0140-6736(00)04046-0
7. Diakos CI, Charles KA, McMillan DC, et al. Cancer-related inflammation and treatment effectiveness. *Lancet Oncol*. 2014;15(11):e493–e503. doi:10.1016/S1470-2045(14)70263-3
8. Candido J, Hagemann T. Cancer-related inflammation. *J Clin Immunol*. 2013;33(Suppl 1):S79–S84. doi:10.1007/s10875-012-9847-0
9. Mantovani A, Allavena P, Sica A, et al. Cancer-related inflammation. *Nature*. 2008;454(7203):436–444. doi:10.1038/nature07205
10. Rui LX, Shu SY, Jun WJ, et al. The dual induction of apoptosis and autophagy by SZC014, a synthetic oleanolic acid derivative, in gastric cancer cells via NF-kappaB pathway. *Tumour Biol*. 2016;37:5133–5144. doi:10.1007/s13277-015-4293-2
11. Shishodia S, Koul D, Aggarwal BB. Cyclooxygenase (COX)-2 inhibitor celecoxib abrogates TNF-induced NF-kappa B activation through inhibition of activation of I kappa B alpha kinase and Akt in human non-small cell lung carcinoma: correlation with suppression of COX-2 synthesis. *J Immunol*. 2004;173:2011–2022. doi:10.4049/jimmunol.173.3.2011

12. Lin EY, Pollard JW. Tumor-associated macrophages press the angiogenic switch in breast cancer. *Cancer Res*. 2007;67:5064–5066. doi:10.1158/0008-5472.CAN-07-0912
13. Han TS, Hur K, Xu G, et al. MicroRNA-29c mediates initiation of gastric carcinogenesis by directly targeting ITGB1. *Gut*. 2015;64:203–214. doi:10.1136/gutjnl-2013-306640
14. Hu Y, Liu JP, Li XY, et al. Downregulation of tumor suppressor RACK1 by Helicobacter pylori infection promotes gastric carcinogenesis through the integrin beta-1/NF-kappaB signaling pathway. *Cancer Lett*. 2019;450:144–154. doi:10.1016/j.canlet.2019.02.039
15. Zhu S, Soutto M, Chen Z, et al. Helicobacter pylori-induced cell death is counteracted by NF-kappaB-mediated transcription of DARPP-32. *Gut*. 2017;66:761–762. doi:10.1136/gutjnl-2016-312141
16. Liang H, Kim YH. Identifying molecular drivers of gastric cancer through next-generation sequencing. *Cancer Lett*. 2013;340:241–246. doi:10.1016/j.canlet.2012.11.029
17. Giraud AS, Menheniott TR, Judd LM. Targeting STAT3 in gastric cancer. *Expert Opin Ther Targets*. 2012;16:889–901. doi:10.1517/14728222.2012.709238
18. Judd LM, Bredin K, Kalantzis A, et al. STAT3 activation regulates growth, inflammation, and vascularization in a mouse model of gastric tumorigenesis. *Gastroenterology*. 2006;131(4):1073–1085. doi:10.1053/j.gastro.2006.07.018
19. Guo T, Liu Z-L, Zhao Q, et al. A combination of astragaloside I, levistilide A and calycosin exerts anti-liver fibrosis effects in vitro and in vivo. *Acta Pharmacol Sin*. 2018;39(9):1483–1492. doi:10.1038/aps.2017.175
20. Zhang YY, Tan RZ, Zhang XQ, et al. Calycosin ameliorates diabetes-induced renal inflammation via the NF-kappaB pathway in vitro and in vivo. *Med Sci Monit*. 2019;25:1671–1678. doi:10.12659/MSM.915242
21. Wang Q, Lu W, Yin T, et al. Calycosin suppresses TGF-beta-induced epithelial-to-mesenchymal transition and migration by upregulating BATF2 to target PAI-1 via the Wnt and PI3K/Akt signaling pathways in colorectal cancer cells. *J Exp Clin Cancer Res*. 2019;38:240. doi:10.1186/s13046-019-1243-7
22. Qiu R, Li X, Qin K, et al. Antimetastatic effects of calycosin on osteosarcoma and the underlying mechanism. *Biofactors*. 2019;45:975–982. doi:10.1002/biof.1545
23. Nie XH, Ou-yang J, Xing Y, et al. Calycosin inhibits migration and invasion through modulation of transforming growth factor beta-mediated mesenchymal properties in U87 and U251 cells. *Drug Des Devel Ther*. 2016;10:767–779. doi:10.2147/DDDT.S90457
24. Zhou L, Wu Y, Guo Y, et al. Calycosin enhances some chemotherapeutic drugs inhibition of Akt signaling pathway in gastric cells. *Cancer Invest*. 2017;35:289–300. doi:10.1080/07357907.2016.1278226
25. Cai T, Zhang C, Zhao Z, et al. The gastric mucosal protective effects of astragaloside IV in mnng-induced GPL rats. *Biomed Pharmacother*. 2018;104:291–299. doi:10.1016/j.biopha.2018.04.013
26. Zeng J, Yan R, Pan H, et al. Weipixiao attenuate early angiogenesis in rats with gastric precancerous lesions. *BMC Complement Altern Med*. 2018;18:250. doi:10.1186/s12906-018-2309-3
27. Zhang C, Cai T, Zeng X, et al. Astragaloside IV reverses MNNG-induced precancerous lesions of gastric carcinoma in rats: regulation on glycolysis through miRNA-34a/LDHA pathway. *Phytother Res*. 2018;32:1364–1372. doi:10.1002/ptr.6070
28. Chen Z, Zhu S, Hong J, et al. Gastric tumour-derived ANGPT2 regulation by DARPP-32 promotes angiogenesis. *Gut*. 2016;65:925–934. doi:10.1136/gutjnl-2014-308416
29. Zhu S, Soutto M, Chen Z, et al. Activation of IGF1R by DARPP-32 promotes STAT3 signaling in gastric cancer cells. *Oncogene*. 2019;38:5805–5816. doi:10.1038/s41388-019-0843-1
30. Smolinska M, Grzanka D, Antosik P, et al. HER2, NF-kappaB, and SATB1 expression patterns in gastric cancer and their correlation with clinical and pathological parameters. *Dis Markers*. 2019;2019:6315936. doi:10.1155/2019/6315936
31. Correa P. Human gastric carcinogenesis: a multistep and multifactorial process–first American cancer society award lecture on cancer epidemiology and prevention. *Cancer Res*. 1992;52:6735–6740.
32. Sung JK. Diagnosis and management of gastric dysplasia. *Korean J Intern Med*. 2016;31:201–209. doi:10.3904/kjim.2016.021
33. Xu ZY, Chen JS, Shu YQ. Gene expression profile towards the prediction of patient survival of gastric cancer. *Biomed Pharmacother*. 2010;64:133–139. doi:10.1016/j.biopha.2009.06.021
34. Zhao ZS, Li L, Wang HJ, et al. Expression and prognostic significance of CEACAM6, ITGB1, and CYR61 in peripheral blood of patients with gastric cancer. *J Surg Oncol*. 2011;104:525–529. doi:10.1002/jso.21984
35. Uhm JH, Gladson CL, Rao JS. The role of integrins in the malignant phenotype of gliomas. *Front Biosci*. 1999;4:D188–D199. doi:10.2741/Uhm
36. Park CC, Bissell MJ, Barcellos-Hoff MH. The influence of the microenvironment on the malignant phenotype. *Mol Med Today*. 2000;6:324–329. doi:10.1016/S1357-4310(00)01756-1
37. Weaver VM, Lelievre S, Lakins JN, et al. beta4 integrin-dependent formation of polarized three-dimensional architecture confers resistance to apoptosis in normal and malignant mammary epithelium. *Cancer Cell*. 2002;2:205–216. doi:10.1016/S1535-6108(02)00125-3
38. Karin M. NF-kappaB as a critical link between inflammation and cancer. *Cold Spring Harb Perspect Biol*. 2009;1:a000141. doi:10.1101/cshperspect.a000141
39. Sokolova O, Naumann M. NF-kappaB signaling in gastric cancer. *Toxins (Basel)*. 2017;9. doi:10.3390/toxins9040119
40. HW PH L, Zhao ZM, Shi YF, et al. Effect of weipixiao on plasma tumor necrosis factor alpha and interleukin-4 expression in rats with gastric precancerous lesions. *J Guangzhou Univ Trait Chin Med*. 2015;32:271–274.
41. Kawamura T, Endo Y, Yonemura Y, et al. Significance of integrin alpha2/beta1 in peritoneal dissemination of a human gastric cancer xenograft model. *Int J Oncol*. 2001;18:809–815.
42. El-Rifai W, Smith MF Jr, Li G, et al. Gastric cancers overexpress DARPP-32 and a novel isoform, t-DARPP. *Cancer Res*. 2002;62:4061–4064.
43. Mukherjee K, Peng D, Brifkani Z, et al. Dopamine and cAMP regulated phosphoprotein MW 32 kDa is overexpressed in early stages of gastric tumorigenesis. *Surgery*. 2010;148:354–363. doi:10.1016/j.surg.2010.05.011
44. Alvero AB, Chen R, Fu HH, et al. Molecular phenotyping of human ovarian cancer stem cells unravels the mechanisms for repair and chemoresistance. *Cell Cycle*. 2009;8:158–166. doi:10.4161/cc.8.1.7533
45. Ji Y, Wang Z, Li Z, et al. Angiotensin II induces angiogenic factors production partly via AT1/JAK2/STAT3/SOCS3 signaling pathway in MHCC97H cells. *Cell Physiol Biochem*. 2012;29(5–6):863–874. doi:10.1159/000171034
46. Zhao M, Gao FH, Wang JY, et al. JAK2/STAT3 signaling pathway activation mediates tumor angiogenesis by upregulation of VEGF and bFGF in non-small-cell lung cancer. *Lung Cancer*. 2011;73:366–374. doi:10.1016/j.lungcan.2011.01.002
47. Atkinson GP, Nozell SE, Benveniste ET. NF-kappaB and STAT3 signaling in glioma: targets for future therapies. *Expert Rev Neurother*. 2010;10:575–586. doi:10.1586/ern.10.21
48. Yu H, Pardoll D, Jove R. STATs in cancer inflammation and immunity: a leading role for STAT3. *Nat Rev Cancer*. 2009;9:798–809.
49. Wang XY, Wang LL, Zheng X, et al. Expression of p-STAT3 and vascular endothelial growth factor in MNNG-induced precancerous lesions and gastric tumors in rats. *World J Gastrointest Oncol*. 2016;8:305–313. doi:10.4251/wjgo.v8.i3.305
50. Yu H, Jove R. The STATs of cancer–new molecular targets come of age. *Nat Rev Cancer*. 2004;4:97–105. doi:10.1038/nrc1275
51. Bromberg J, Wang TC. Inflammation and cancer: IL-6 and STAT3 complete the link. *Cancer Cell*. 2009;15:79–80. doi:10.1016/j.ccr.2009.01.009

52. McFarland BC, Gray GK, Nozell SE, et al. Activation of the NF-kappaB pathway by the STAT3 inhibitor JSI-124 in human glioblastoma cells. *Mol Cancer Res*. 2013;11:494–505. doi:10.1158/1541-7786.MCR-12-0528
53. Lentsch AB, Ward PA. Regulation of inflammatory vascular damage. *J Pathol*. 2000;190:343–348. doi:10.1002/(SICI)1096-9896(200002)190:3<343::AID-PATH522>3.0.CO;2-M
54. Whiteford JR, De Rossi G, Woodfin A. Mutually supportive mechanisms of inflammation and vascular remodeling. *Int Rev Cell Mol Biol*. 2016;326:201–278.
55. Bid HK, Oswald D, Li C, et al. Anti-angiogenic activity of a small molecule STAT3 inhibitor LLL12. *PLoS One*. 2012;7:e35513. doi:10.1371/journal.pone.0035513
56. Huang C, Jiang T, Zhu L, et al. STAT3-targeting RNA interference inhibits pancreatic cancer angiogenesis in vitro and in vivo. *Int J Oncol*. 2011;38:1637–1644. doi:10.3892/ijo.2011.1000
57. Qian WF, Guan WX, Gao Y, et al. Inhibition of STAT3 by RNA interference suppresses angiogenesis in colorectal carcinoma. *Braz J Med Biol Res*. 2011;44:1222–1230. doi:10.1590/S0100-879X2011007500143
58. Efferth T, Shan L, Zhang ZW. Tonic Herbs and Herbal Mixtures in Chinese Medicine. *World J Tradit Chin Med*. 2016;1 :10-25. doi:10.15806/j.issn.2311-8571.2015.0037
59. Divi RL, Chang HC, Doerge DR. Anti-thyroid isoflavones from soybean: isolation, characterization, and mechanisms of action. *Biochem Pharmacol*. 1997;54:1087–1096. doi:10.1016/S0006-2952(97)00301-8
60. Sartelet H, Serghat S, Lobstein A, et al. Flavonoids extracted from fonio millet (Digitaria exilis) reveal potent antithyroid properties. *Nutrition*. 1996;12:100–106. doi:10.1016/0899-9007(96)90707-8